PERGAMON

Chemical Engineering Science 58 (2003) 747–758

Chemical Engineering Science

www.elsevier.com/locate/ces

Design of a prototype miniature bioreactor for high throughput automated bioprocessing

S. R. Lamping[a], H. Zhang[a], B. Allen[b], P. Ayazi Shamlou[a,*]

[a] *Department of Biochemical Engineering, University College London, Torrington Place, London, WC1E 7JE, UK*
[b] *Eli Lilly and Company, Lilly Corporate Center, Indianapolis, Indiana 46285, USA*

Abstract

A new miniature bioreactor with a diameter equal to that of a single well of a 24-well plate is described and its engineering performance as a fermenter assessed. Mixing in the miniature bioreactor is provided by a set of three impellers mechanically driven via a microfabricated electric motor and aeration is achieved with a single tube sparger. Parameter sensitive fluorophors are used with fibre optic probes for continuous monitoring of dissolved oxygen tension and an optical based method is employed to monitor cell biomass concentration during fermentation. Experimental measurements are provided on volumetric mass transfer coefficient for air–water and bacterial fermentation data are presented for *Escherichia coli*.

The local and average power input, energy dissipation rate and bubble size are derived from an analysis of the multiphase flow in the miniature bioreactor using computational fluid dynamics (CFD). Volumetric mass transfer coefficients are predicted using Higbie's penetration model with the contact time obtained from the CFD simulations of the turbulent flow in the bioreactor. Comparative data are provided from parallel experiments carried out in a 20 l (15 l working volume) conventional fermenter. Predicted and measured volumetric mass transfer coefficients in the miniature bioreactor are in the range 100–400 h^{-1}, typical of those reported for large-scale fermentation.

1. Introduction

The realisation that there are approximately 30,000 genes in the human genome has shifted drug discovery research significantly towards proteomics and away from genomics. Currently, the available drugs on the market target nearly 500 of the estimated hundreds of thousands of human proteins with the expectation that this number will increase by a factor of 10–100 in the next few years. A major challenge for drug discovery now is to elucidate the relationship between proteins produced by each gene and disease. In this respect, advances in proteomics and automated high-throughput screening based on the shaken microwell plate system have provided the technology platform for a significant increase in the number of potential drug candidates that are likely to come forward. A related challenge that is yet to be addressed is the need to define the conditions for the translation of results from the microwell system to conventional laboratory scale. For example, in the case of *Escherichia coli* fermentation, while a number of discovery companies now routinely run fermentation in a 24-well plate to produce small quantities of proteins for crystallographic studies, scale-up to laboratory fermentation, typically up to 10 l, is proving difficult to achieve. The ability to scale-up such information and the capacity to generate process data from unit operations carried out at the microwell scale have become important issues in the development pathway of a new drug. This has provided the motivation for a few recent studies on microwell scale bioprocessing, including the present investigation the aim of which is to describe the engineering design of a miniature bioreactor and assess its use as a fermenter.

Shaken flask fermentation, with working volumes between 50 and 500 ml, has been used with very little change for over five decades for cell growth culture, media screening and cell expansion (Kato, Hiraoka, Tada, Lee, & Koh, 1999; Buchs, 2001; Rhodes & Gaden, 1957; Maier & Buchs, 2001). "Instrumented" shake flasks have been used recently to establish bulk mixing and oxygen transfer in these systems and work is in progress to establish the relationships

* Corresponding author. Tel.: +44-20-7679-3841; fax: +44-20-7679-3943.
E-mail address: p.shamlou@ucl.ac.uk (P. Ayazi Shamlou).

0009-2509/03/$ - see front matter
doi:10.1016/S0009-2509(02)00604-8

between these parameters and cell growth and product yields (Anderlei & Buchs, 2001; Weuster-Botz, Altenbach-Rehem, & Arnold, 2001).

The automated shaken microwell system has been used in a few of recent publications to obtain process information on biological materials. These include studies on bacterial fermentation (Weiss, John, Klimant, & Heinzle, 2001b; Duetz et al., 2000; Duetz & Witholt, 2001), animal cell cultures (Girard, Jordan, Tsao, & Wurm, 2001) and biotransformation (Doig, Pickering, Lye, & Woodley, 2001; Weiss, John, Klimant, & Heinzle, 2001a). As far as oxygen transfer is concerned, the limited data available indicate that the volumetric mass transfer coefficient in a shaken microwell (Weiss, John, Klimant, & Heinzle, 2001b) is likely to be lower, by at least a factor of 10, compared to a conventional scale fermenter. Walther et al. (1994) have described a miniature bioreactor with a working volume of 3 ml for cell culture in a space laboratory and Kostov, Harms, Randers-Eichhorn, and Rao (2001) have recently presented the design of a microreactor with a working volume of 2 ml and reported basic data on the responses of pH, dissolved oxygen and optical density probes using *E. coli* fermentation as a test bed. Mixing was achieved by the action of a magnetic stirrer placed at the bottom of the well. Initial results demonstrated that fermentation at the microwell-scale was feasible, but achieving adequate overall oxygen transfer rate in the microreactor proved difficult and comparison of K_La with data from a 1 l conventional fermenter showed the difficulties in using magnetic-bar stirrer in the microreactor.

In the present study, we report engineering data to demonstrate the operation of a new miniature bioreactor having a diameter equal to that of a single well of a standard 24-well plate. A microfabricated three-bladed turbine impeller was used to mix the contents of the miniature bioreactor and a single sparger placed underneath the bottom impeller provided the means for aeration. Microfabricated fibre optic probes (Junker, Wang, & Hatton, 1988; Wang, Shahriari, & Mosrris, 1999) were used for in situ measurement of process parameters including dissolved oxygen, pH and cell density. Volumetric oxygen transfer data were obtained for air–water and *E. coli* fermentations for different operational conditions. The results were compared with data obtained from parallel experiments using a 20 l mechanically agitated fermenter with a working volume of 15 l and with predictions from theory based on CFD simulations of multiphase flow in the miniature bioreactor and the Higbie's penetration model for mass transfer.

2. Materials and methods

The miniature bioreactor: Fig. 1 shows the main elements of the miniature bioreactor together with some of its associated instrumentation and interconnections. The bioreactor was machined from Plexiglas to allow visual inspection of mixing and gas bubbles. Air–water was used to establish the engineering performance of the miniature bioreactor for mass transfer operations and *E. coli* DH5α was chosen as a fermentation system because of its robustness and tolerance to contamination. Subsequent miniature bioreactors in our laboratory (not described here) are built from stainless steel with parts that can be fully sterilised for cell culture experiments.

The cylindrical chamber of the miniature bioreactor was 16 mm in diameter and 48 mm high (working volume of 6 ml). The mixing of the contents of the bioreactor was achieved by means of three, 6-bladed open flat-turbine impellers, each having a diameter of 7.0 mm and width of 1.5 mm. The impellers were driven from the top of the bioreactor with a microfabricated electric motor (Smoovy, Switzerland) with a shaft diameter of 1 mm and an infinitely variable speed control (maximum speed and torque of 15,000 rpm and 2.2 m Nm, respectively). The bottom impeller was placed approximately 6 mm from the base of the chamber, the distance between two impellers was 7.5 mm and the distance between the top impeller and the free liquid surface was 7.0 mm. The bioreactor was equipped with four baffles of width 1.8 mm and thickness 0.6 mm. The air from a compressed air supply was sparged through a perforated plastic cap placed at the discharge tip of a single tube of internal diameter 1.0 mm. The sparger was placed directly beneath the hub of the bottom impeller (Fig. 1). The air flow rate was measured using a standard laboratory rotameter with a flow rate in the range of 0.2–100 ml min^{-1} of air (Barnant Company, IL, USA). The gas supply had a separate connection via a two-way valve to a compressed nitrogen cylinder allowing mass transfer experiments to be carried out as described later in this section.

On-line measurements of dissolved oxygen tension, pH, and cell density were performed by means of fibre optic probes; temperature was measured by means of a fine diameter copper-constantine thermocouple. The oxygen sensor, the optrode (fibre optic oxygen sensor, AVS-OXYKIT 1.5, Knight Optical Technologies Ltd., Surrey, UK) consisted of a 1 mm diameter silica glass optical fibre sealed in a 7 cm long stainless steel tube rod. The working tip of the probe was dip-coated with a ruthenium complex immobilised in a sol–gel matrix. An optical fibre carried light from a blue LED [470 nm output peak] to the immobilised ruthenium/sol–gel coating layer at the working tip of the stainless-steel tube. The 470 nm light excites the ruthenium complex to fluoresce. The level of this fluorescence is quenched in the presence of oxygen molecules, which diffuse through the sol–gel matrix and interact with the trapped ruthenium. The reduction in the fluorescence signal is related to the concentration of oxygen through the Stern–Volmer equation (Wang et al., 1999). The level of fluorescence signal was detected using a second fibre optic, part of the integrated optical probe and the fluorescence light was analysed by a sensitive CCD detector array grating spectrometer (Type: AVS-MC2000; Knight Optical Technologies Ltd.; www.knightoptech.com). This

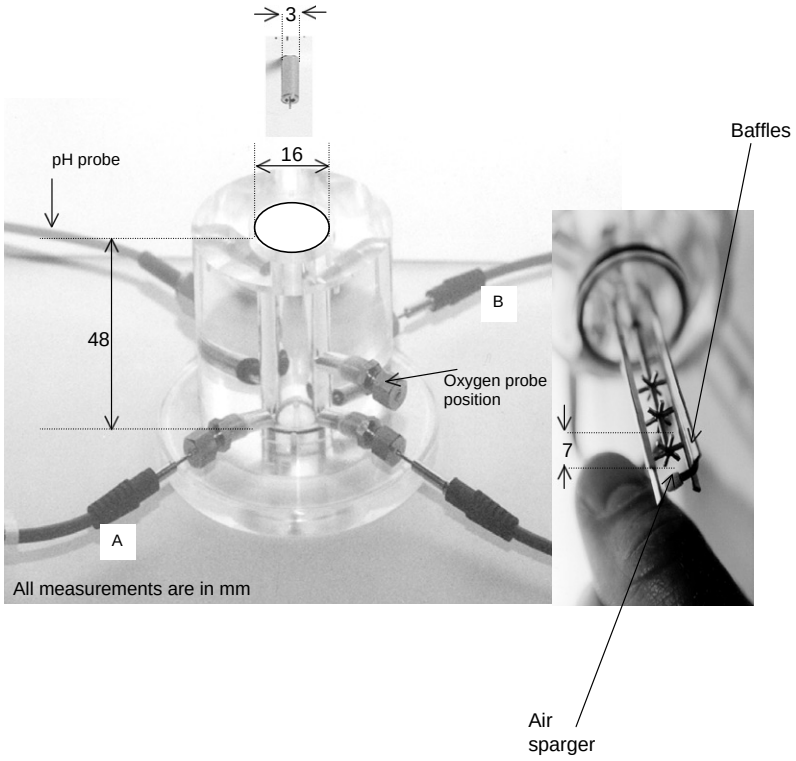

Fig. 1. Main components of the miniature bioreactor. All measurements are in mm.

has multiple spectrometer channels for other parallel spectral sensors, such as pH, turbidity, and other fluorescence investigations as described below. The primary channel for oxygen was used to monitor both LED light source excitation level and fluorescence emission simultaneously capturing full spectra in milliseconds.

In the present study, solution pH was measured by an optical probe using the method of Junker et al. (1988). The pH sensor consisted of: a fibre optic probe of diameter 1.5 mm (FCR-UV200F, Knight Optical Technologies Ltd., Surrey, UK); a xenon pulsed light source (XE-2000) and a blue LED light source (LED-475) coupled to a multiple channel spectrometer (MC2000). The fluorophor, 1-hydroxypyrene-3,6,8-trisulfonic acid trisodium salt (HPTS, Sigma-Aldrich, Dorset, England) with a pK_a value of 7.3 was selected for the experiments described here. Two different excitation wavelengths of 405 and 460 nm were used. The fluorescence intensity was measured at a single emission wavelength of 520 nm. A linear calibration curve was obtained in 20 g l^{-1} of HPTS in water using the method of (Junker et al., 1988). The spectrometer was used to monitor the change in fluorescence.

The measurement of cell density was achieved by combining three optical fibre probes, as shown in Fig. 1. Each fibre was fabricated from a single 600 μm active core diameter fibre. One fibre was used to deliver the light produced by a miniature tungsten light source to the bioreactor contents. The other two probes were used for light collection from the bioreactor, one for transmitted light (625 nm) and one for scattered light. This arrangement allowed a range of measurements including turbidity, transmission/colour and nephelometry to be carried out by a multiple channel spectrometer (MC2000). In the present study the broth turbidity was sufficiently low to allow reliable cell density data to be obtained from the measurement of transmitted light (probes A and B).

Air–water experiments: The performance of the miniature bioreactor was assessed initially under defined flow conditions through a series of experiments carried out with air–water. The results from these experiments also allowed a basis for comparison with conventional bioreactors for which many correlations are available (Smith, Van't Riet, & Middleton, 1977; Van't Riet, 1979; Ni, Gao, Cumming, & Pritchard, 1995). K_La values were calculated from the dissolved oxygen concentration profiles obtained as a function of time by using the dynamic gassing out technique (Van't Riet, 1979). Before each experiment, the optrode was calibrated at 100% and 0% air saturation by sparging air and nitrogen, respectively. A typical experiment started with fresh de-ionised water containing a known amount of sodium chloride salt and with the impeller speed set at a predetermined value. The oxygen concentration was continuously monitored as a function of time. Nitrogen was sparged till the level of oxygen had fallen to zero. At this point, the gas supply was switched rapidly to air set at a fixed flow rate of 1 vvm corresponding to a superficial

velocity of 0.0005 m s^{-1} and the rise in oxygen concentration was monitored.

Fermentation: All fermentations in the miniature bioreactor were carried out with *E. coli*, DH5α in batch mode at 37°C, an air flow rate of 1 vvm at impeller speeds 1300, 1500 and 1850 rpm. No attempt was made in these experiments to optimise the fermentation process, the aim was to demonstrate that fermentation was achievable in the miniature bioreactor and obtain basic engineering and fermentation parameters for comparison with conventional scale fermentation. Data for the latter were obtained in a 20 l (15 l working volume) LH20L03 HI-CAT series bioreactor (Adaptive Biosystems Ltd., Progress Business Park, Luton, UK). pH was fixed at the start of fermentation, but not controlled.

The cultures were grown on a semi-defined medium which consisted of, per litre, D-glucose (10 g), $MgSO_4 \cdot 7H_2O$ (1.2 g), $(NH_4)_2SO_4$ (4 g), KH_2PO_4 (13.3 g), citric acid (1.7 g), Na_2EDTA (8.4 mg), $CoCl_2 \cdot 6H_2O$ (2.5 mg), $MnSO_4 \cdot 4H_2O$ (15 mg), $CuSO_4 \cdot 2H_2O$ (1.5 mg), H_3BO_3 (3 mg), $NaMoO_4 \cdot 2H_2O$ (2.5 mg), ZnCl (13 mg), Fe (III) citrate (100 mg), thiamine hydrochloride (4.5 mg; Sigma-Aldrich, Fancy Road, Poole, UK) and casamino acids (10 g l^{-1}; Oxoid). The pH of the medium was adjusted to 6.3 prior to sterilisation by addition of 4 M NaOH. All chemicals were obtained from BDH (Dorset, England) unless otherwise stated. Sterilisation of the miniature bioreactor was achieved by rinsing the equipment with 1 M NaOH followed by sterile water. Seed culture was prepared by inoculating 10 ml of the medium in a McCartney bottle with a single colony from nutrient agar plates. The culture was allowed to grow overnight at 37°C and rotated at 200 rpm by a horizontal shaken platform in an incubator. 10 ml of seed culture was used to inoculate 500 ml of fresh medium, which was grown for 6 h under the same conditions. The 500 ml culture was used as the starting point for all experiments in the miniature bioreactor and the 20 l fermenter. In the case of the miniature bioreactor, 0.6 ml of the culture was used to inoculate 5.4 ml of fresh medium in the bioreactor. A 10% inoculation was also used for the 20 l fermentation. In the large fermenter foaming was controlled automatically by the addition of 100% polypropylene glycol (PPG) pumped at a concentration of 0.1 ml l^{-1}. The 20 l bioreactor was operated in the batch mode and the initial fermentation conditions were as follows: temperature, 37°C; air flow, 1 vvm (12 l min^{-1}); DO_2, 100%; agitator speed, 530 rpm; pH 6.3. The aeration and agitation were kept constant throughout the fermentation. Oxygen levels were monitored using an Ingold polarographic probe (Mettler-Toledo Ltd., Beaumont Leys, Leicester, UK). Online data were logged by Propack data logging and acquisition software (Acquisition Systems, Fleet, Hampshire, UK). Cultures were grown for 14 h.

Simulation of flow in the miniature bioreactor: Energy dissipation rate gas volume fraction and air–liquid interfacial area are important engineering flow parameters used in correlating experimental K_La data. In the present study the power input, and hence energy dissipation rate, to the microimpellers could not be measured with confidence because of the very low values of torque involved. The power input was predicted as part of an analysis of the multiphase flow and mixing in the miniature bioreactor by using computational fluid dynamics, CFD (CFX 4.1, AEA Technology, UK). The standard Reynolds-Averaged-Navier–Stokes (RANS) model was used to solve the three-dimensional two-phase (gas–liquid) turbulent flow in the miniature bioreactor and the closure of the problem was achieved using the $k-\varepsilon$ model. Turbulent kinetic energy, k, and energy dissipation, ε, were obtained from the homogeneous model, where k and ε were assumed to be the same for both phases throughout the vessel (Soon, Harbridge, Titchener-Hooker, & Ayazi Shamlou, 2000; Boychyn et al., 2001). The motion of the gas bubbles and their interaction with the flowing liquid were described in terms of the drag force acting on the bubbles, the impact of lift force and the virtual mass effects were ignored. The gas and liquid momentum equations were coupled by the interfacial force terms due to the drag force by the following equation:

$$F_\alpha = -F_\beta = 0.75 r_\alpha \rho_\alpha \frac{C_d}{d_b} |U_\beta - U_\alpha| (U_\beta - U_\alpha). \quad (1)$$

The drag coefficient C_d was determined from the modified Reynolds number (Kuo & Wallis, 1988) and the interaction between bubbles were taken into account by making use of the correlation proposed by Ishii and Zuber (1979) for the drag force in a bubble swarm. The impeller was described by the inclusion of additional source terms in the momentum equations using the method of Pericleous and Patel (1987). Each baffle was treated as a thin surface and described by defining an appropriate time-averaged sink term in the momentum equations as using recommended previously (Morud & Hjertager, 1996; Revstedt, Fuchs, & Tragardh, 1998; Xu & McGrath, 1996).

The average bubble size was estimated from the following correlation (Wilkinson, Vanschayk, Spronken, Laurent, & Van Dierendonck, 1993):

$$d = \left(\frac{We_c \sigma}{\rho_\alpha} \right)^{0.6} \varepsilon^{(-0.4)}. \quad (2)$$

The critical Weber number, We_c, in Eq. (2) was assumed to have a value equal to 0.6 (Hinze, 1955). The energy dissipation term, ε, in Eq. (2) was based on flow conditions around the impeller blades, and considering the small size of the miniature bioreactor, bubble coalescence was assumed to be negligible. For both phases, no-slip boundary conditions were applied. Free-slip conditions were used along the bottom and side walls (Morud & Hjertager, 1996). The gas sparger was simulated as a solid body. The gas inlet was set on top plane of the solid body and the normal component of gas was specified according to the gas flow rate (1 vvm). At

gas outlet (top of the vessel), the velocity was determined from a mass balance based on inlet conditions. For a fixed impeller speed and gas flow rate, the CFD simulations provided the distribution of the relevant engineering parameters in the miniature bioreactor including the velocity field, bubble size, gas hold-up, and the energy dissipation rates. The local values of the energy dissipation rates were integrated over the vessel volume to obtain an average value over the entire contents. The average power input was obtained directly from the integrated energy dissipation rate and used for comparison with published data. The simulated parameters were also used in a mass transfer model to predict both the profile and the integrated overall mass transfer coefficient, K_La, as described later on in section under results and discussion.

3. Results and discussions

Mixing and flow in the miniature bioreactor: The CFD simulations of speed and energy dissipation rate for a single phase liquid with the properties of water are shown in Fig. 2 for a speed of 2500 rpm. The single-phase power number, N_p, was obtained by integrating the simulated local energy dissipation rates over the entire volume of the vessel and dividing it by the group $\rho_l N^3 D^5$. Thus:

$$Np = \frac{2\int r_\alpha \rho_\alpha \varepsilon \, \mathrm{d}V}{\rho_\alpha N^3 Di^5}, \tag{3}$$

where r_α is the local liquid fraction which was taken to be equal to 1.0 for the case of single (liquid) phase, and the local fluid density ρ_α was assumed to be liquid density, ρ_l. The simulated impeller power curve was obtained by assuming equal distribution of power input between the three impellers. These simulations predicted a power number of approximately 4.0 for the microimpeller in turbulent flow regime, comparable to published experimental values for a large-scale unit with similar configuration (Uhl & Gray, 1966). Eq. (3) was also used to predict the local and average power input for the two-phase, gas–liquid system, in the miniature bioreactor (simulations not shown). The results gave a ratio of gassed to ungassed power, P_g/P, of 0.8–0.9. The reported ratio of P_g/P varies between 0.9 and 0.4 depending on the type of impeller and gas flow number (Smith et al., 1977).

Flow simulations were also performed for the 20 l standard fermenter equipped with a set of three Rushton turbines. The CFD simulated single-phase power curve predicted a power number 6.0 for turbulent flow which compared favourably with published values for the Rushton turbine impeller (Uhl & Gray, 1966).

For distilled water an average value of 4×10^{-4} m s^{-1} has been recommended for liquid mass transfer coefficient, K_L and solution ionic strength is known to increase the overall volumetric mass transfer coefficient, K_La, partly through its impact on interfacial area, a (Van't Riet, 1979). The effect of ions on K_La however is not easy to predict, but according to experimental information it varies with the type of ions present in solution and is dependent on the prevailing fluid energy dissipation rates. Van't Riet's (1979) analysis of the published experimental data indicate that such uncertainties coupled with different measurement techniques mean that reported empirical correlations are likely to vary in their estimations of K_La by up to ±40%. Higbie's (1935) penetration model of mass transfer at a gas–liquid interface has been used previously to describe mass transfer in air-lifts (Ayazi Shamlou, Pollard, & Ison, 1995) and mechanically agitated mixing vessels (Kawase & Moo-Young, 1990). According to Higbie's model, mass transfer at a gas–liquid interface is assumed to occur by a series of encounters between the liquid and the gas. Each encounter lasts for only a short time so that steady-state conditions are never established and any mass transfer that occurs is due to the unsteady molecular diffusion. The relationship between the mass transfer coefficient, K_L, liquid-phase diffusivity, ξ, and exposure time, t, is given by

$$K_L = \frac{2}{\pi^{1/2}}\left(\frac{\xi}{t}\right)^{1/2}. \tag{4}$$

In a mechanically agitated vessel, Kolmogoroff's theory of homogeneous and isotropic turbulence has been used to obtain the following equation for the surface renewal time, t, as follows:

$$t = \left(\frac{v}{\varepsilon}\right)^{1/2}, \tag{5}$$

where the local energy dissipation rate, ε, is obtained from the CFD simulation of flow in the vessel.

Combining Eqs. (4) and (5) and rearranging it leads to the following equation for the local liquid phase mass transfer coefficient, K_L.

$$K_L(r,z,\theta) = \frac{2}{\pi^{1/2}}[\varepsilon(r,z,\theta)v]^{1/4}\left(\frac{\xi}{v}\right)^{-1/2}. \tag{6}$$

The local specific surface area available for mass transfer is given by:

$$a(r,z,\theta) = \frac{6r_\beta(r,z,\theta)}{d_b}, \tag{7}$$

where r_β is the local gas volume fraction. We used Eqs. (5) and (6) to predict the K_La distributions in the miniature bioreactor. Fig. 3 shows the distribution of gas volume fraction and K_La in the vessel for air–water. The profiles shown in Fig. 3 are for a speed of 2500 rpm and an air flow rate of 1 vvm. To compare these predictions with experimental data, the overall (average) volumetric mass transfer coefficient was calculated by integrating the local values over the entire working volume of the miniature bioreactor.

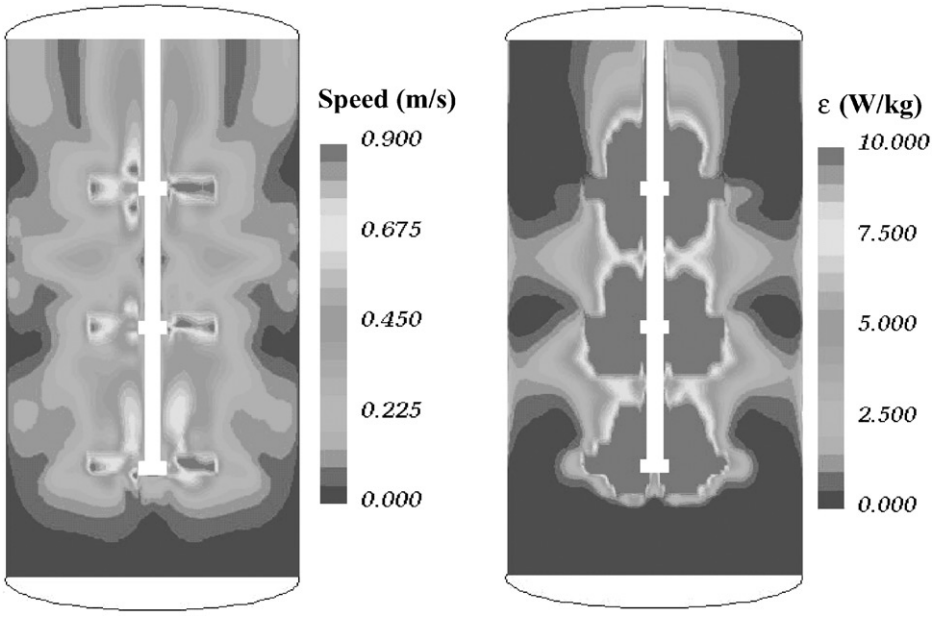

Fig. 2. CFD simulations of distributions of liquid speed and energy dissipation rate in the miniature bioreactor for an impeller speed of 2500 r.p.m. Liquid properties are assumed to be those of water.

Thus

$$K_L a = \frac{\int K_L(r,z,\theta)a(r,z,\theta)\,\mathrm{d}v}{V}. \tag{8}$$

The overall $K_L a$ were predicted for a range of impeller speeds and the operational airflow rate of 1 vvm used in our experiments. The results are presented and discussed below.

Air–water $K_L a$ results: The experimental $K_L a$ values were based on the well-mixed model for both the gas and liquid phases, as suggested by Dunn and Einsele (1975). The well-mixed model is considered appropriate for this case because of the small size of the miniature bioreactor. According to this model, $K_L a$ is obtained from the oxygen probe response data by the following expression:

$$K_L a = \frac{1}{t}\ln\left(\frac{C^*}{C^* - C}\right) = \frac{1}{t}\ln\left(\frac{1}{C_L}\right), \tag{9}$$

where C_L is a normalized oxygen concentration defined by: $C_L = (C* - C)/C$.

The optrode used in the present investigation had a response time, τ_p(the time needed to record 63% of a stepwise change), of 42 s at 20°C, measured using a standard procedure described elsewhere (Dunn & Einsele, 1975). CFD predictions gave an overall volumetric mass transfer coefficient, $K_L a$, in the miniature bioreactor typically in the order of 100 h^{-1} (0.03 s^{-1}) indicating that the impact of the probe response time on $K_L a$ was an important consideration. We used a first-order response model recommended by Badino, Facciotti, & Schmidell (2001) in our calculations to account for the fibre optic probe response time. Thus,

$$\frac{\mathrm{d}C_p}{\mathrm{d}t} = \frac{1}{\tau_p}(C_L - C_P), \tag{10}$$

where C_p is the normalized dissolved oxygen concentration measured by the probe. Substituting for C_L using Eq. (7), integrating and rearranging gives the following expression for $K_L a$:

$$C_P = \frac{1}{t_m - \tau_p}\left[t_m \exp\left(\frac{-t}{t_m}\right) - \tau_p \exp\left(\frac{-t}{\tau_p}\right)\right], \tag{11}$$

where $t_m = 1/K_L a$. Eq. (11) was solved for $K_L a$ using Microsoft Excel at each time measurement and the results averaged. $K_L a$ data were obtained for air–water in the presence of sodium chloride for a range of impeller speeds. Fig. 4 shows the results plotted as a function of the mean energy dissipation rate in the miniature bioreactor. For comparison, selected CFD simulated values of $K_L a$ are also shown. The continuous line in Fig. 4 shows the predicted $K_L a$ based on the correlation of Van't Riet (1979). The slope of the best line of fit through the data points has a slope which agrees well with the 0.7, which is the exponent of (P/V) in the equation reported by Van't Riet (1979). However, the absolute values of $K_L a$ measured in our experiments are consistently lower by approximately 40% compared to those expected from Van't Riet's expression. The difference is thought to be due to the differences in the vessel-impeller configuration between the two systems. Van't Riet's equation is based on data obtained for standard a Rushton turbine impeller, which is more efficient than the open flat turbine configuration used in the present study. It is

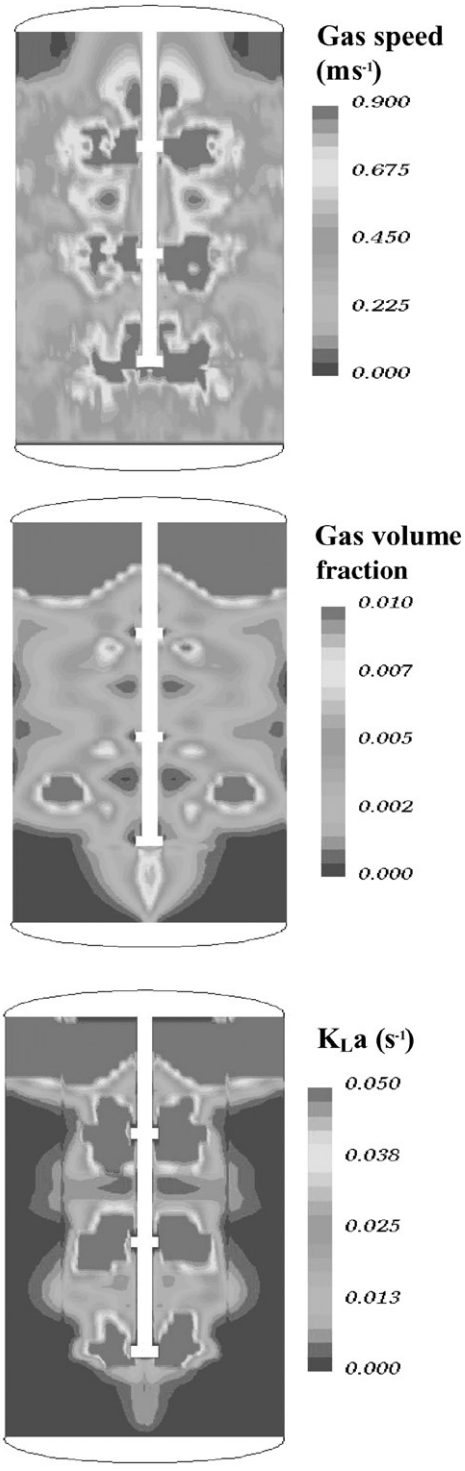

Fig. 3. CFD simulations of distributions of gas speed, gas volume fraction and K_La in the miniature bioreactor for an impeller speed of 2500 r.p.m and air flow rate of 1 v.v.m. Liquid properties are assumed to be those of salt-water.

notable that CFD-predicted K_La values are in good agreement with experimental K_La data, at least in the range of power per unit volume examined ($5 \times 10^2 < P/V < 5 \times 10^4$ W m^{-3}), which covers the range of interest to most fermentations.

We carried out additional experiments using the standard 20 l (working volume, 15 l) bioreactor in which we measured K_La for air–water as a function of impeller speed. The airflow rate in the 20 l bioreactor was set at 1 vvm, equivalent to 0.007 m s^{-1} (compared to 0.0005 m s^{-1} in the miniature bioreactor). To compare the results for the two bioreactors therefore the overall volumetric mass transfer coefficient data for the each reactor were adjusted by assuming $K_La \propto v_s^{0.2}$, as recommended by Van't Riet (1979). The results are shown in Fig. 5 where the solid line was obtained from Van't Riet's equation and the dashed-lines represent ±40% deviations from it. The K_La values for the miniature bioreactor consistently fall below those of the 20 l fermenter, but the best lines of fit through the data points for the two scales have the same slope which very close to the exponent of P/V in Van't Riet's equation. It is also notable that while the K_La data for the miniature bioreactor are lower than the 20 l scale the difference are within the expected 40% deviation. Taken together the observations based on Figs. 4 and 5 support the view that the engineering performance of the miniature bioreactor is adequately described by current CFD techniques and that its performance, at least as far as mixing and oxygen transfer is concerned, matches those of laboratory bioreactors.

E. coli K_La and fermentation results: Figs. 6a and b show respectively the variation of dissolved oxygen and dry cell weight (g l^{-1}) as a function of time for fermentation of *E. coli*, DH5α, in the miniature bioreactor. The profiles shown in Figs. 6a and b are used routinely to monitor the progress of fermentation and provide data for calculation of other important fermentation parameters including oxygen uptake rate. These aspects are beyond the scope of this investigation, the aim of which is to compare the performance of the miniature bioreactor with a large fermenter. The data in Figs. 6a and b refer to experiments carried out at a fixed impeller speed of 1500 rpm corresponding to a simulated mean energy dissipation rate, ε, of 0.53 W kg^{-1}. In each case data are also shown from parallel experiments carried out in the 20 l fermenter using standard probes and running under normal fermentation conditions described in Section 2. Fluorescence-based fibre optic probes, for monitoring of fermentation parameters including pH and dissolved oxygen, have been fully described and successfully tested previously (Junker et al., 1988). In the case of pH, we used both a pH indicator dye immobilised on the working tip of the fibre optic probe, as well as the HPTS dye directly introduced into the culture medium. The former is preferable but in our experiments we found its response to be very slow and erratic (data not shown). In contrast acceptable results were obtained from the probe responding to the dissolved HPTS dye. In the case of oxygen, the response of the commercial immobilised fluorophore probe was reliable and its calibration reproducible. No attempt was made in these experiments to run the fermentations in the two scales

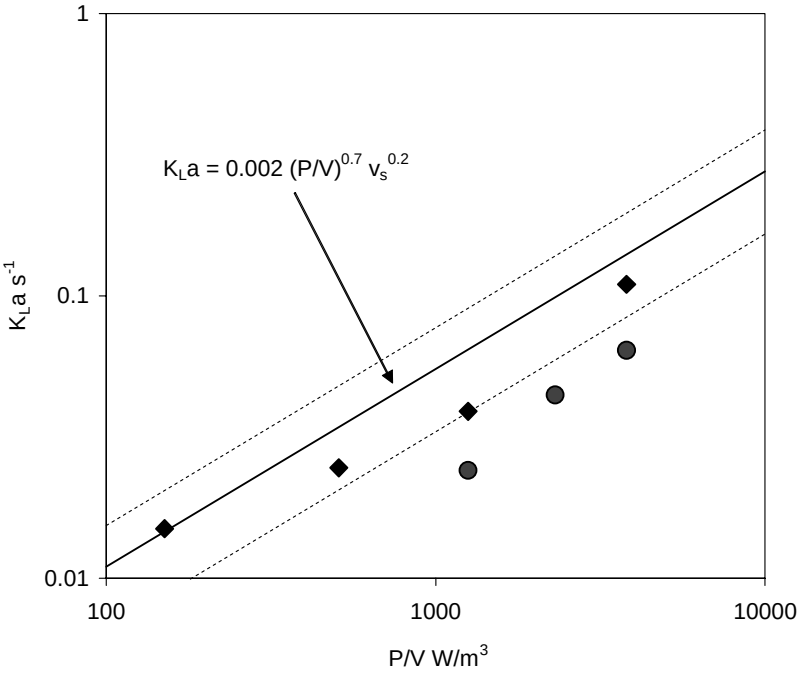

Fig. 4. Overall volumetric mass transfer coefficient as a function of the impeller power input per unit volume. The plots are for the miniature bioreactor and refer to air–water system: (♦) are experimental data and (●) are the values obtained from CFD simulations. The solid line is the relationship reported by Van't Riet (1979) based on a comprehensive review of K_La data for Rushton turbine impellers. The dashed lines are the ±40% deviation from Van't Riet's equation due to experimental uncertainties and different measurement techniques.

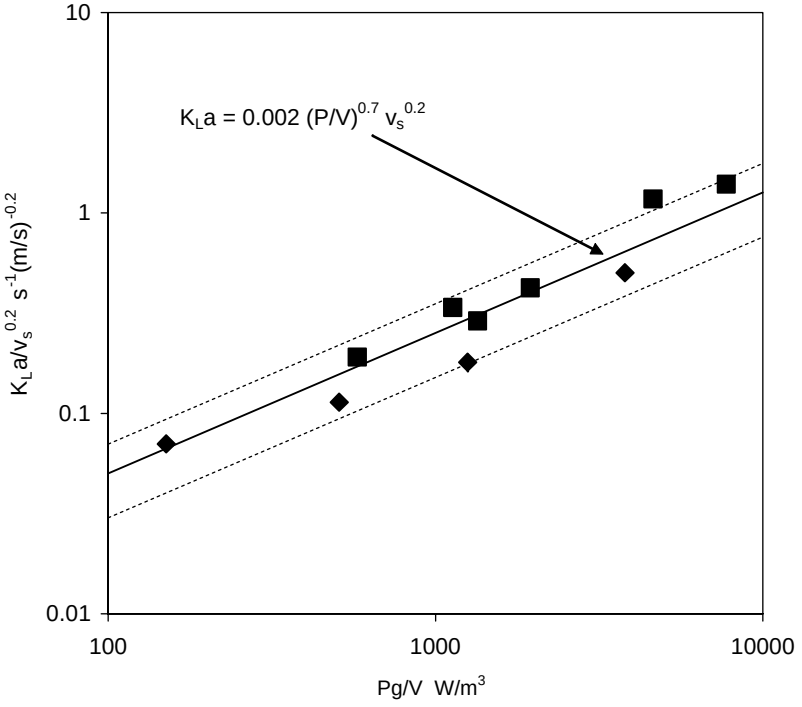

Fig. 5. Overall volumetric mass transfer coefficients (♦) for the miniature bioreactor compare well with those obtained in a 20 l (15 l working volume) (■) fermenter. Data refer to air–water. The two scales were operated at different superficial gas velocities and the data for the two scales were brought together by assuming $K_La \propto (v_s)^{0.2}$ as recommended by Van't Riet (1979). The solid line and the dashed lines are explained in caption for Fig. 4.

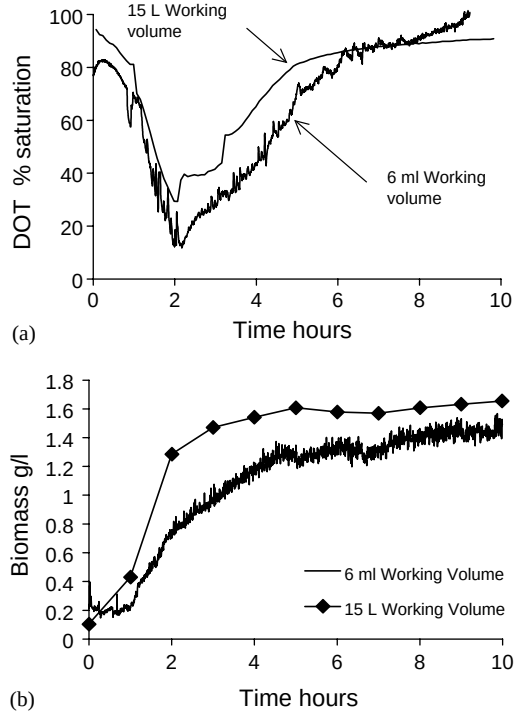

Fig. 6. The fibre optic response curves for the dissolved oxygen (6a) and biomass Concentration (6b) obtained in the miniature bioreactor are compared with profiles obtained in a 20 l (15 l working volume) fermenter. The data were obtained during fermentation of *E coli*. No attempt was made to run the fermentation in the miniature bioreactor under the optimum conditions. The difference in profile of the two scales are thought to be due to differences in the geometrical configuration of the two systems.

under comparable conditions. The agreement between the responses of the two probes demonstrated by the data in Figs. 6a and b therefore are encouraging and any differences between the probes are thought to be due to differences in the geometry and operational conditions of the two bioreactors.

Measurements of K_La in the miniature bioreactor were made for two impeller speeds at the end of the fermentation period during the stationary phase. In these experiments care was taken to ensure that during the de-aeration stage in the gassing out method the oxygen concentration did not fall below 30% saturation (Badino et al., 2001). The results are plotted in Fig. 7 where the solid line shows the line of best fit obtained from the air–water experiments. The results indicate that volumetric mass transfer coefficients in the miniature fermenter fall within the range reported for conventional mechanically agitated bioreactors. It is notable that the concept of power input per unit volume as a scale-up parameter successfully links the performance of the miniature bioreactor to conventional fermenter. Kostov et al. (2001) have provided K_La data for a magnetically stirred 2 ml miniature bioreactor equipped with optical probes. Using *E. coli* fermentation, values of K_La of 9.8, 27.5 and 44.4 h^{-1} were reported for air flow rate of 1, 2 and 3 vvm. These K_La values are similar to those reported recently by Duetz et al. (2000) for air–water and are lower than values observed typically in shake flasks and conventional mechanically stirred systems. By comparison K_La values measured during *E. coli* fermentation in our turbine-stirred miniature bioreactor at a fixed aeration rate of 1 vvm were 68 and 128 h^{-1} at power input per unit volume of 413 and 1190 Wm^{-3}, respectively. These are well within the range of values observed in conventional mechanically agitated systems as shown in Figs. 4, 5 and 7 reported in the literature for air–water (Van't Riet, 1979).

One practical problem with our current oxygen sensor is its relatively long response time. The Perspex bioreactor used in the present study necessitated the elimination of the effect of external light on the response of the probes during measurements. To achieve this the whole bioreactor was rapped in a layer of thin aluminium foil during the experiments and the immobilised tip of the oxygen sensor was covered with an extra coating of silicon. The presence of this extra coating on the working tip of probe caused the observed increase in its response time. The new miniature bioreactors in our laboratory are now fabricated from stainless steel such that their contents are fully isolated from external lighting. Another consideration is the need to control the temperature of the broth in the miniature bioreactor during fermentation. In the present study, this was achieved by carrying out the experiments in an incubator. Having established the "proof of concept" in the present study, in the new design, broth temperature will be controlled by the insertion of a single miniature concentric cylinder tubular heat exchanger fabricated from stainless steel.

Challenging the miniature bioreactor: Having established the engineering parameters that define the performance of the miniature bioreactor, we used it to explore new process situations. Our future plan of work includes a detailed comparison of the performance of shaken microwell systems for gas–liquid contacting operations measured against the performance of the miniature bioreactor. In shaken microwell systems, oxygen transfer is normally achieved by surface aeration. We challenged the miniature bioreactor by running an experiment in which we measured the volumetric oxygen transfer rate, K_La, in water with the supply of air to the sparger turned off so that any oxygen transfer occurred entirely via surface aeration. The results are shown in Fig. 8 for three values of power input per unit volume. The solid line shows the best line of fit for oxygen transfer by aeration through the single tube sparger (see Fig. 4). The relatively low values of K_La observed under the condition of surface aeration suggest that most current shaken microwell systems for fermentation are likely to run under conditions of severe oxygen limitation. We also challenged the miniature bioreactor by running it in a "bubble column" mode, i.e. under conditions where the only form of agitation was provided by the flow of air (zero impeller speed) into the vessel. We measured the overall mass transfer coefficient for an air flow rate of 1 vvm corresponding

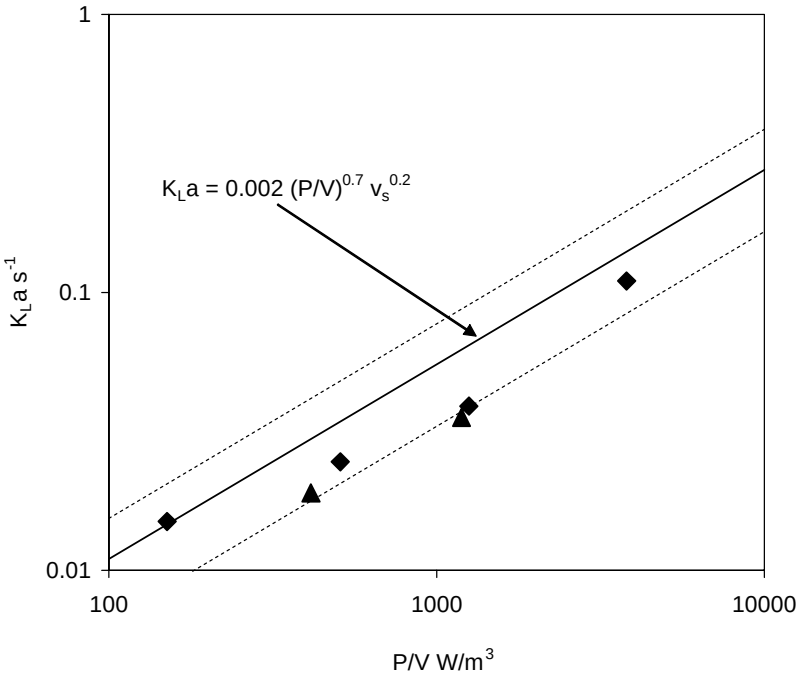

Fig. 7. Overall mass transfer coefficients measured during fermentation of *E. coli* in the miniature bioreactor (▲). The data compare very well with the $K_L a$ obtained for air–water (♦).

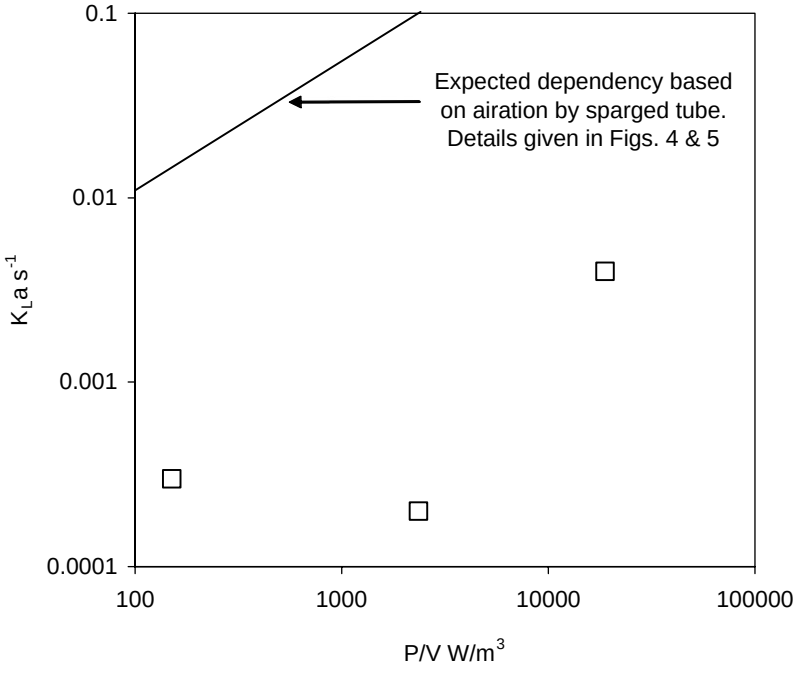

Fig. 8. Overall mass transfer coefficients were measured (×) under conditions of surface aeration only. Significantly lower $K_L a$ data compared to values obtained under aeration via the sparger (solid line) indicate that in microwell scale fermentation in shaken systems involving oxygen demanding microorganisms may be a potential problem.

to the value used in our standard air–water and *E. coli* fermentation experiments. The calculated power input per unit volume for this system was based on the method of Ayazi Shamlou et al. (1995). The overall mass transfer coefficient obtained for this system was 67 h^{-1} comparable to typical values obtained under low agitation ($P/V \leqslant 100$), but significantly higher than what was achievable by surface aeration.

4. Conclusions

In this paper we describe a new miniature gas–liquid bioreactor and use experimental and theoretical analysis to establish its performance as a fermenter. The bioreactor was designed to have the same diameter as that of a single well of a 24-well plate but was mechanically agitated and aerated such that its operation mimicked the flow conditions in a conventional mechanically stirred reactor. The miniature bioreactor was instrumented with microprobes for measurement of fermentation parameters including dissolved oxygen, pH, temperature and optical density. The overall mass transfer coefficient was predicted theoretically from theory and measured in the miniature bioreactor using air–water and *E. coli* fermentation. The results were compared well with data obtained from a 20 l (15 l working volume. The miniature bioreactor was challenged by running it under conditions similar to those in a shaken microwell system. Significantly lower mass transfer rates were observed highlighting the potential of oxygen starvation during fermentation in most current microwell systems.

Notation

A	gas–liquid interfacial area, $m^2\ m^{-3}$
C_d	drag coefficient
C, C_L, C^*, C_p	oxygen concentration, mol m^{-3}
d_b	bubble diameter, m
D_i	impeller diameter, m
F	drag force, N
k	turbulent kinetic, $m^2\ s^{-2}$
K_L	liquid phase mass transfer coefficient, $m\ s^{-1}$
n_b	bubble population density, m^3
N	rotational speed, s
N_p	impeller power number,
P	impeller power input, W
r	volume fraction, radial co-ordinate
t	surface renewal time, s
t	time, s
t_m	mass transfer time, s
T	tank diameter, m
$\mathbf{U}$	velocity, $m\ s^{-1}$
v_s	superficial gas velocity, $m\ s^{-1}$
V	volume, m^3
We	dimensionless Weber number
z	axial co-ordinate

Greek letters

α	liquid phase
β	gas phase
ε	turbulent energy dissipation, $m^2\ s^{-3}$
θ	angular co-ordinate
μ	viscosity, kg $(m\ s)^{-1}$
ν	kinematic viscosity, $m^2\ s^{-1}$
ξ	liquid diffusivity, $m^2\ s^{-1}$
ρ	density, kg m^{-3}
σ	surface tension, kg $(m^{-2}\ s)^{-1}$
τ_p	probe response time, s

Acknowledgements

UCL is the EPSRC's Innovative Manufacturing Centre in Bioprocessing (IMRC). The Council's support is greatly acknowledged. The authors are grateful to John Knight of Knight Optical Technologies for advice on the on the use of fibre optic probes and to Alison Key for valuable help on the fermentation. SRL is an EPSRC EngD student sponsored by Eli Lilly and HZ's work is supported by a UCL ORS award and a KC Wong Scholarship.

References

Anderlei, T., & Buchs, J. (2001). Device for sterile online measurements of oxygen transfer rate in shaking flasks. *Biochemical Engineering Journal*, *7*, 157–162.

Ayazi Shamlou, P., Pollard, D. J., & Ison, A. P. (1995). Volumetric mass transfer coefficient in concentric-tube airlift bioreactors. *Chemical Engineering Science*, *50*, 1579–1590.

Badino, A. C., Facciotti, M. C. R., & Schmidell, W. (2001). Volumetric oxygen transfer coefficients (K_La) in batch cultivations involving non-Newtonian broths. *Biochemical Engineering Journal*, *8*(2), 111–119.

Boychyn, M.Y., Yim, S.S.S., Ayazi Shamlou, P., Bulmer, P., More, J., & Hoare, M. (2001). Characterisation of flow intensity in continuous centrifuges for the development of laboratory mimics. *Chemical Engineering Science*, *56*, 4759–4770.

Buchs, J. (2001). Introduction to advantages and problems of shaken cultures. *Biochemical Engineering Journal*, *7*, 91–98.

Doig, S. D., Pickering, S. C. R., Lye, G. J., & Woodley, J. M. (2001). The use of microscale processing technologies for quantification of biocatalytic Baeyer–Villiger oxidation kinetics. *Biotechnology and Bioengineering*, *80*, 42–49.

Duetz, W. A., Ruedi, L., Hermann, R., O'Connor, K., Buchs, J., & Witholt, B. (2000). Methods for intense aeration, growth, storage and replication of bacterial strains in microtitre plates. *Applied Environmental Microbiology*, *66*, 2641–2646.

Duetz, W. A., & Witholt, B. (2001). Effectiveness of orbital shaking for the aeration of suspended bacterial cultures in square-deepwell microtitre plates. *Biochemical Engineering Journal*, *7*, 113–115.

Dunn, I. J., & Einsele, A. J. (1975). Oxygen transfer coefficients by the dynamic method. *Journal of Applied Chemistry & Biotechnology*, *25*, 707–720.

Girard, P., Jordan, M., Tsao, M., & Wurm, F. M. (2001). Small-scale bioreactor system for process development and optimization. *Biochemical Engineering Journal*, *7*, 117–119.

Higbie, R. (1935). Rate of absorption of a pure gas into a still liquid during short periods of exposure. *Trans. AIChE*, *31*, 365–389.

Hinze, J. O. (1955). Fundamentals of the hydrodynamic mechanism of splitting in dispersion process. *A.I.Ch.E. Journal*, *1*, 289–295.

Ishii, M., & Zuber, N. (1979). Drag coefficient and relative velocity in bubbly, droplet or particulate flows. *A.I.Ch.E. Journal*, *25*, 843–855.

Junker, B. H., Wang, D. I. C., & Hatton, T. A. (1988). Fluoresence sensing of fermentation parameters using fibre optics. *Biotechnology and Bioengineering*, *32*, 55–63.

Kato, Y., Hiraoka, S., Tada, Y., Lee, Y.-S., & Koh, S.-T. (1999). Performance of a shaking vessel with current pole. *3rd International symposium on mixing in industrial processes*, Osaka, Japan, pp. 349–356.

Kawase, Y., & Moo-Young, M. (1990). Mathematical models for design of bioreactors: Applications of Kolmogoroff's theory of isotropic turbulence. *Chemical Engineering Journal*, *43*, B19–B41.

Kostov, Y., Harms, P., Randers-Eichhorn, L., & Rao, G. (2001). Low-cost microbioreactor for high-throughput bioprocessing. *Biotechnology and Bioengineering*, *72*, 346–352.

Kuo, J. T., & Wallis, G. B. (1988). Flow of bubbles through nozzles. *International Journal of Multiphase Flows*, *14*(5), 547–564.

Maier, U., & Buchs, J. (2001). Characterisation of the gas–liquid mass transfer in shaking bioreactors. *Biochemical Engineering Journal*, *7*, 99–106.

Morud, K. E., & Hjertager, B. H. (1996). LDA measurements and CFD modelling of gas–liquid flow in a stirred vessel. *Chemical Engineering Science*, *51*(2), 233–249.

Ni, X., Gao, S., Cumming, R. H., & Pritchard, D. W. (1995). A comparative study of mass transfer in yeast for a batch pulsed baffled bioreactor and a stirred tank fermenter. *Chemical Engineering Science*, *50*, 2127–2136.

Pericleous, K. A., & Patel, M. K. (1987). The modeling of tangential and axial agitation in chemical reactors. *PCH Physiochemical Hydrodynamics*, *8*(2), 105–123.

Revstedt, J., Fuchs, L., & Tragardh, C. (1998). Large eddy simulation of the turbulent flow in a stirred reactor. *Chemical Engineering Science*, *53*(24), 4041–4053.

Rhodes, R. P., & Gaden Jr., R. P. (1957). Characterisation of agitation effects in shaken flasks. *Industrial Engineering Chemistry*, *49*, 1233–1236.

Smith, J. M., Van't Riet, K., & Middleton, J. C. (1977). Scale-up of agitated gas–liquid reactors for mass transfer. *2nd European conference on mixing*, Cambridge, UK, pp. (F4) 51–(F4) 66.

Soon, S. Y., Harbridge, J., Titchener-Hooker, N., & Ayazi Shamlou, P. (2000). Prediction of drop breakage in an ultra high velocity jet homogeniser. *Journal of Chemical Engineering Japan*, *34*(5), 640–646.

Uhl, V. W., & Gray, J. B. (1966). *Mixing—theory and practice*, Vol. 1. New York: Academic Press, pp. 133.

Van't Riet, K. (1979). Review of measuring methods and results in nonviscous gas–liquid mass transfer in stirred vessels. *Industrial and Engineering, Chemistry, Process Design and Development*, *18*, 357–364.

Walther, I., van der Schoot, B. H., Jeanneret, S., Arquint, P., de Rooij, V. F., Gass, V., Bechler, B., Lorenzi, G., & Cogoli, A. (1994). Development of a miniature bioreactor for continuous culture in a space laboratory. *Journal of Biotechnology*, *38*, 21–32.

Wang, W., Shahriari, M., & Mosrris, M. J. (1999). Applying fibre-optic sensors for monitoring dissolved oxygen. *SEA Technology*, *40*, 69–74.

Weiss, S., John, G. t., Klimant, I., & Heinzle, E. (2001a). Towards pH control in 96-well microtitreplates. *10th European congress biotechnology*, Spain (8–11 July), p. 199.

Weiss, S., John, G. t., Klimant, I., & Heinzle, E. (2001b). Mixing and oxygen transfer in microtitreplates, http://www.biovt.rwth-aachen.de/ast2001/program/abstract/abstract11.htm.

Weuster-Botz, D., Altenbach-Rehem, J., & Arnold, M. (2001). Parallel substrate feeding and pH-control in shaking-flasks. *Biochemical Engineering Journal*, *7*, 163–170.

Wilkinson, P. M., Vanschayk, M., Spronken, J. P. M., Laurent, L., & Van Dierendonck, L. T. (1993). The influence of gas density and liquid properties on bubble break-up. *Chemical Engineering Science*, *48*(7), 1213–1226.

Xu, Y., & McGrath, G. (1996). CFD predictions of stirred tank flows. *Transactions of the Institution of Chemical Engineers*, *74*(A), 471–475.